Capillary Break-up Rheometry of Low-Viscosity Elastic Fluids

Lucy E. Rodd[1,3], Timothy P. Scott[3], Justin J. Cooper-White[2], Gareth H. McKinley[3]*

[1] Department of Chemical and Biomolecular Engineering, The University of Melbourne, VIC 3010, Australia

[2] Division of Chemical Engineering, The University of Queensland, Brisbane, QLD 4072, Australia

[3] Hatsopoulos Microfluids Laboratory, Department of Mechanical Engineering, Massachusetts Institute of Technology, Cambridge, MA 02139, USA

*Email: gareth@mit.edu

Received: 9.8.2004, Final version: 11.11.2004

Abstract:
We investigate the dynamics of the capillary thinning and break-up process for low viscosity elastic fluids such as dilute polymer solutions. Standard measurements of the evolution of the midpoint diameter of the necking fluid filament are augmented by high speed digital video images of the break up dynamics. We show that the successful operation of a capillary thinning device is governed by three important time scales (which characterize the relative importance of inertial, viscous and elastic processes), and also by two important length scales (which specify the initial sample size and the total stretch imposed on the sample). By optimizing the ranges of these geometric parameters, we are able to measure characteristic time scales for tensile stress growth as small as 1 millisecond for a number of model dilute and semi-dilute solutions of polyethylene oxide (PEO) in water and glycerol. If the final aspect ratio of the sample is too small, or the total axial stretch is too great, measurements are limited, respectively, by inertial oscillations of the liquid bridge or by the development of the well-known beads-on-a-string morphology which disrupt the formation of a uniform necking filament. By considering the magnitudes of the natural time scales associated with viscous flow, elastic stress growth and inertial oscillations it is possible to construct an “operability diagram” characterizing successful operation of a capillary break-up extensional rheometer. For Newtonian fluids, viscosities greater than approximately 70 mPas are required; however for dilute solutions of high molecular weight polymer, the minimum viscosity is substantially lower due to the additional elastic stresses arising from molecular extension. For PEO of molecular weight $2 \cdot 10^6$ g/mol, it is possible to measure relaxation times of order 1 ms in dilute polymer solutions with zero-shear-rate viscosities on the order of 2 – 10 mPas.

Zusammenfassung:
Wir untersuchen die Dynamik der Kapillarverdünnung und des Zerreissens niedrig-viskoser elastischer Fluide wie verdünnte Polymerlösungen. Die standardisierten Messungen der Veränderung des Durchmessers in der Mitte des einschnürenden flüssigen Filaments werden durch Hochgeschwindigkeitsdigitalvideoaufnahmen der Zerreissdynamik verbessert. Wir zeigen, dass eine erfolgreiche Bedienung eines Kapillarverdünnungsgeräts von drei wichtigen Zeitskalen bestimmt wird (die die relative Bedeutung von trägen, viskosen und elastischen Prozessen charakterisieren), und darüber hinaus von zwei wichtigen Längenskalen (die die Ausgangsgrösse der Probe und das Verstreckverhältnis der Probe spezifizieren). Durch Optimierung dieser geometrischen Parameter sind wir in der Lage, die charakteristischen Zeitskalen des Zugspannungswachstums bis 1 ms für mehrere Modelllösungen aus Polyethylenoxid (PEO) in Wasser und Glyzerin zu messen. Wenn das Aspektverhältnis der Probe zu klein ist oder die absolute axiale Verstreckung zu gross, werden die Messungen durch Trägheitsoszillationen der flüssigen Brücke oder der Entwicklung der bekannten Perlen-auf-der-Kette-Morphologie begrenzt, die die Bildung eines gleichmässig einschnürenden Filaments verhindern. Durch Betrachtung der Grösse der natürlichen Zeitskalen, die mit dem viskosen Fliessen, dem Wachstum der elastischen Spannungen und den Trägheitsoszillationen verbunden sind, ist es möglich, ein "Bedienungsdiagramm" zu erstellen, das die erfolgreiche Bedienung eines Kapillaraufbruchdehnrheometers darstellt. Für Newtonsche Fluide sind Viskositäten grösser als ca. 70 mPas erforderlich; für verdünnte Lösungen von hochmolekularen Polymeren ist die minimale Viskosität jedoch wesentlich kleiner aufgrund der zusätzlichen elastischen Spannungen, die aus der molekularen Verstreckung resultieren. Für PEO mit Molekulargewicht 2 x 10**6 g/mol ist es möglich, Relaxationszeiten in der Grössenordnung von 1 ms in verdünnten Polymerlösungen mit Schernullviskositäten der Grössenordnung von 2 – 10 mPas.

Résumé:
Nous avons étudié la dynamique des mécanismes d’amincissement et de rupture capillaire dans le cas de fluides élastiques de faible viscosité tels que des solutions diluées de polymère. Des mesures standard de l’évolution du diamètre médian du filament de fluide sous striction sont augmentées par des images vidéo digitalisées

à grande vitesse qui rendent compte de la dynamique de rupture. Nous montrons que le fonctionnement correct d'un appareil d'amincissement capillaire est gouverné par 3 échelles de temps importantes (qui caractérisent l'importance relative des mécanismes inertiels, visqueux et élastiques), et aussi par deux longueurs caractéristiques importantes (qui spécifient la taille initiale de l'échantillon et l'étirement total imposé à l'échantillon). En optimisant les portées de ces paramètres géométriques, nous sommes capable de mesurer des montées en contrainte de tension sur des échelles de temps aussi petites que la microseconde, pour un certain nombre de solutions standards diluées et semi diluées d'oxyde de polyéthylène (PEO) dans de l'eau et du glycérol. Si le rapport d'anisotropie de l'échantillon est trop petit, ou si l'étirement axial est trop grand, alors les mesures sont limitées respectivement par les oscillations inertielles du pont liquide ou par le développement de la célèbre morphologie de perles-sur-une-corde qui empêche la formation d'un filament de constriction uniforme. En considérant les ordres de grandeur des échelles de temps naturel associés avec l'écoulement visqueux, la montée en contrainte élastique et les oscillations inertielles, il est possible de construire un «diagramme d'opérabilité» qui caractérise le bon fonctionnement d'un rhéomètre extensionnel à rupture de capillaire. Pour des fluides Newtoniens, des viscosités supérieures à environ 70mPa sont requises; cependant pour les solutions diluées de polymères de haut poids moléculaire, la viscosité minimale autorisée est significativement plus petite, à cause des contraintes élastiques additionnelles qui ont pour origine l'extension moléculaire. Pour un PEO possédant un poids moléculaire de 2×10^6 g/mol, il est possible de mesurer des temps de relaxation de l'ordre de la milliseconde pour des solutions diluées possédant une viscosité statique de l'ordre de 2-10 mPa.s.

Key words: capillary thinning, extensional rheometry, viscoelastic filament

1 INTRODUCTION

Over the past 15 years capillary break-up elongational rheometry has become an important technique for measuring the transient extensional viscosity of non-Newtonian fluids such as polymer solutions, gels, food dispersions, paints, inks and other complex fluid formulations. In this technique, a liquid bridge of the test fluid is formed between two cylindrical test fixtures as indicated schematically in Fig. 1a. An axial step-strain is then applied which results in the formation of an elongated liquid thread. The profile of the thread subsequently evolves under the action of capillary pressure (which serves as the effective 'force transducer') and the necking of the liquid filament is resisted by the combined action of viscous and elastic stresses in the thread.

In the analogous step-strain experiment performed in a conventional torsional rheometer, the fluid response following the imposition of a step shearing strain (of arbitrary magnitude γ_0) is entirely encoded within a material function referred to as the relaxation modulus $G(t, \gamma_0)$. By analogy, the response of a complex fluid following an axial step strain is encoded in an apparent transient elongational viscosity function $\eta_E(\dot{\epsilon}, t)$ which is a function of the instantaneous strain rate, $\dot{\epsilon}$ and the total Hencky strain ($\epsilon = \int \dot{\epsilon}\, dt'$) accumulated in the material. An important factor complicating the capillary break-up technique is that the fluid dynamics of the necking process evolve with time and it is essential to understand this process in order to extract quantitative values of the true material properties of the test fluid. Although this complicates the analysis, and results in a time-varying extension rate, this also makes the capillary thinning and breakup technique an important and useful tool for measuring the properties of fluids that are used in free-

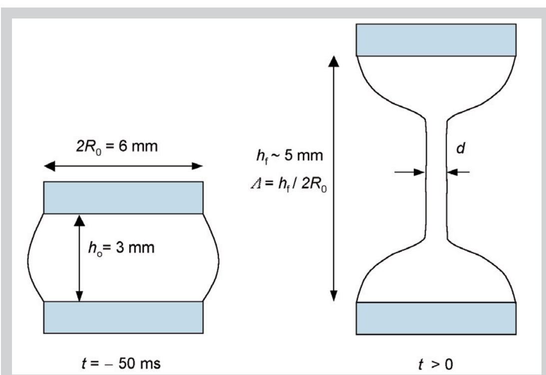

Figure 1: Schematic of the Capillary Breakup Extensional Rheometer (CaBER) geometry containing a fluid sample a) at rest and b) undergoing filament thinning for t > 0.

surface processes such as spraying, roll-coating or ink-jetting. Well-characterized model systems (based on aqueous solutions of polyethylene oxide) have been developed for studying such processes in the past decade and we study the same class of fluids in the present study [1, 2].

Significant progress in the field of capillary break-up rheometry has been made in recent years since the pioneering work of Entov and coworkers [3, 4]. Capillary thinning and break-up has been used to measure quantitatively the viscosity of viscous and elastic fluids [5, 6]; explore the effects of salt on the extensional viscosity for important drag-reducing polymers and other ionic aqueous polymers [7, 8], monitor the degradation of polymer molecules in elongational flow [4] and the concentration dependence of the relaxation time of polymer solutions [9]. The effects of heat or mass transfer on the time-dependent increase of the extensional viscosity resulting from evaporation of a volatile solvent in a liquid adhesive have also been considered [10]; and more recently the extensional rheology of numerous inks and paint dispersions have been studied using capillary thinning rheometry [11]. The relative merits of the capillary break-up elongational rheometry technique (or CABER) and filament stretching elongational rheometry (or FISER) have been discussed by McKinley [12] and a detailed review of the dynamics of capillary thinning of viscoelastic fluids is provided elsewhere [13].

Measuring the extensional properties of low-viscosity fluids (with zero-shear-rate viscosities of $\eta_0 \leq 100$ mPa s, say) is a particular challenge. Fuller and coworkers [14] developed the opposed jet rheometer for studying low viscosity non-Newtonian fluids, and this technique has been used extensively to measure the properties of various aqueous solutions (see for example Hermansky et al. [15] or Ng et al. [16]). Large deformation rates (typically greater than 1000 s^{-1}) are required to induce significant viscoelastic effects, and at such rates inertial stresses in the fluid can completely mask the viscoelastic stresses resulting from molecular deformation and lead to erroneous results [17]. Analysis of jet break-up [18, 19] and drop pinch-off [20, 21] have also been proposed as a means of studying the transient extensional viscosity of dilute polymer solutions. After the formation of a neck in the jet or in the thin ligament connecting a falling drop to the nozzle, the dynamics of the local necking processes in these geometries are very similar to that in a capillary break-up rheometer. However, the location of the neck or 'pinch-point' is spatially-varying and high speed photography or video-imaging is required for quantitative analysis. One of the major advantages of the CABER technique is that the minimum radius is constrained by geometry (and by the initial step-strain) to be close to the midplane of the fluid thread, unless very large axial strains are employed and gravitational drainage becomes important [22].

For low viscosity non-Newtonian fluids such as dilute polymer solutions, the filament thinning process in CABER is also complicated by the effects of fluid inertia which can lead to the well-known beads-on-a-string morphology [23, 24]. Stelter et al. [7] note that such processes prevent the measurement of the extensional viscosity for some of their lowest viscosity solutions. With the increasingly widespread adoption of the CABER technique, it becomes important to understand what range of working fluids can be studied in such instruments. If the fluid is not sufficiently viscous then the liquid thread undergoes a rapid capillary break-up process before the plates are completely separated. The subsequent thinning of the thread can thus not be monitored. The threshold for onset of this process depends on the elongational viscosity of the test fluid and is frequently described qualitatively as 'spinnability' or 'stringiness'. The transient elongational stress growth in the test fluids depends on the concentration and molecular weight of the polymeric solute as well as the background viscosity and thermodynamic quality of the solvent. In the present note we investigate the lower limits of the CABER technique using dilute solutions of polyethylene oxide (PEO) in water and water-glycerol mixtures. In order to reveal the dynamics of the break-up process we combine high-speed digital video-imaging with conventional laser micrometer measurements of the midpoint radius $R_{mid}(t)$. We explore the consequences of different experimental configurations and the roles of solvent viscosity and polymer concentration. The results can be interpreted in terms of an 'operability diagram' based on the viscous and elastic time scales governing the filament thinning process.

2 EXPERIMENTAL METHODS AND DIMENSIONLESS PARAMETERS

2.1 FLUIDS

In this study we have focused on aqueous solutions of a single nonionic polymer; polyethylene oxide (PEO; Aldrich) with molecular weight $M_w = 2.0 \cdot 10^6$ g/mol. Solutions were prepared by mixing the polymer into deionized water at concentrations of 0.10 wt%, and 0.30 wt% using magnetic stirrers at slow/moderate speed settings. In order to explore the effects of the background solvent viscosity, an additional solution with 0.10 wt% PEO dissolved in a mixture of 55% glycerol in water was also prepared. Additional experiments exploring the role of PEO concentration in the Capillary Break-up Rheometer have been performed by Neal and Braithwaite [25]. The results of progressive dilution of a high molecular weight polystyrene dissolved in oligomeric styrene have also been investigated recently using capillary break-up rheometry by Clasen et al. [26]. In this latter study, the solvent viscosity of the oligomer is $\eta_s \geq 40$ Pa s; these solutions are therefore significantly more viscous than the aqueous solutions discussed in the present work.

The important physico-chemical and rheological properties of the test fluids are summarized in Table 1. The steady-shear viscosity of each fluid was measured using a double gap Couette fixture with an AR2000 rheometer. The steady-state values of the surface tension were determined using a Krüss K-10 tensiometer with a platinum du Nouy ring. It is known that aqueous PEO solutions are weakly surface active and that the dynamic surface tension decreases with time after a fresh interface is created [21, 27]. However, the variation in σ is small (typically $\Delta\sigma \leq 10 \cdot 10^{-3}$ N/m) and drop pinch-off/breakup experiments show that this difference does not significantly affect the dominant balance driving the thinning process [27]. We have also performed additional capillary breakup experiments to investigate the role of dynamic surface tension and these are discussed briefly in Section 3.3.

For PEO, the characteristic ratio is $C_\infty = 4.1$ [28], the repeat unit mass is $m_0 = 44$g/mol and the average bond length is $l = 0.147$ nm. The mean square size of an unperturbed Gaussian coil is $\langle R^2 \rangle_0 = C_\infty (3M_w/m_0)^{1/2}$ and we thus obtain $c^* = M_w/(N_A \langle R^2 \rangle_0{}^{3/2}) \approx 2.53 \cdot 10^{-3}$ g/cm^3 for this molecular weight. However, water is known to be a good solvent for PEO, so that the polymer coils are extended beyond the random coil configuration and the above expression is an overestimate of the coil overlap concentration. Tirtaatmadja et al. [27] summarize previous reported values of the intrinsic viscosity for numerous high molecular weight PEO/water solutions. The measurements can be well described by the following Mark-Houwink expression

$$[\eta] = 0.072 M_w^{0.65} \tag{1}$$

with the intrinsic viscosity $[\eta]$ in units of cm^3/g. The solvent quality parameter can be extracted from the exponent in the Mark-Houwink relationship $[\eta] = K\ M_w^{(3\nu-1)}$ to yield $3\nu-1 = 0.65 \Longrightarrow \nu = 0.55$.

Combining this expression with Graessley's expression for coil overlap [29] we find that for our PEO sample $c^* = 0.77/[\eta] \approx 8.6 \cdot 10^{-4}$ g/cm^3 (0.086 wt%). The two solutions considered here are thus weakly semi-dilute solutions.

The longest relaxation time of a monodisperse homopolymer in dilute solution is described by the Rouse-Zimm theory [30] and scales with the following parameters:

Fluid	c/c*	σ [mN/m]	η_0 [mPas]	$t_{Rayleigh}$ [ms]	t_{visc} [ms]	Oh	λ [ms]
0.1wt% PEO	1.16	61.0±0.1	2.3±0.2	20.9	1.61	0.077	1.5
0.3wt% PEO	3.49	60.8±0.2	8.3±1.0	20.8	5.78	0.27	4.4
0.1wt% PEO in Gly/Water	1.16	58.0±0.1	18.2±0.5	23.0	13.3	0.58	23.1

Table 1: The physico-chemical and rheological properties of the aqueous polyethylene oxide (PEO) solutions utilized in the present study. The molecular weight of the solute is $M_w = 2 \cdot 10^6$ g/mol.

$$\lambda \sim \frac{[\eta]\eta_s M_w}{RT} = \frac{K\eta_s M_w^{3\nu}}{RT} \quad (2)$$

where the Mark-Houwink relationship has been used in the second equality. The precise value of the prefactor in the Rouse-Zimm theory depends on the solvent quality and the hydrodynamic interaction between different sections of the chain; however it can be approximately evaluated by the following expression [27]:

$$\lambda = \frac{1}{\zeta(3\nu)} \frac{[\eta]\eta_s M_w}{RT} \quad (3)$$

where

$$\zeta(3\nu) = \sum_{i=1}^{\infty} \frac{1}{i^{3\nu}}$$

represents the summation of the individual modal contributions to the relaxation time. For ν = 0.55 the prefactor is $1/\zeta(3\nu)$ = 0.463. The longest relaxation time for the PEO solutions utilized in the present study is thus λ = 0.34 ms. Christanti and Walker [31] use a different prefactor in Eq. 3 but report very similar values of the Zimm time constant for PEO solutions of the same molecular weight (but in a more viscous solvent).

This value of the relaxation time represents the value obtained under dilute solution conditions and characteristic of small amplitude deformations so that the individual chains do not interact with each other. However the solutions studied in the present experiment are in fact weakly semidilute solutions and the extensional flow in the neck results in large molecular deformations. Numerous recent studies with dilute solutions of high molecular weight polymers [8, 9, 19, 27] have shown that the characteristic viscoelastic time scale measured in filament thinning or drop break-up experiments is typically larger than the Zimm estimate and is concentration dependent for concentration values substantially below c*. The Zimm time-constant should thus be considered as a lower bound on the polymer time scale that is measured during a capillary thinning and break-up experiment.

2.2 INSTRUMENTATION

In the present experiments we have used a Capillary Break-up Extensional Rheometer designed and constructed by Cambridge Polymer Group (www.campoly.com). The diameter of the end plates is D_0 = 6 mm and the final axial separation of the plates can be adjusted from 8 mm to 15 mm. The midpoint diameter is measured using a near-infra-red laser diode assembly (Omron ZLA-4) with a beam thickness of 1mm at best focus and a line resolution of approximately 20 μm. High resolution digital video is recorded using a Phantom V5.0 high speed camera (at 1000 frames/second) with a Nikon 28 - 70 mm f/2.8 lens. Exposure times are 214 μs per frame. The video is stored digitally using an IEEE1394 firewire link and individual frames are cropped to a size of 512 x 216 pixels. The resulting image resolution is 26.8 μm/pixel and the overall image magnification is 1.7 x.

2.3 LENGTH-SCALES, TIME-SCALES AND DIMENSIONLESS PARAMETERS

The operation of a capillary-thinning rheometer is governed by a number of intrinsic or naturally-occurring length and time scales. It is essential to understand the role of these lengthscales and timescales in controlling the dynamics of the thinning and break-up process. We discuss each of these scales individually below:

The Sample Aspect Ratio: $\Lambda(t) = h(t)/2R_0$
As indicated in Fig. 1, the initial sample is a cylinder with aspect ratio $\Lambda_0 = h_0/2R_0$. Exploratory numerical simulations for filament stretching rheometry [32, 33] show that optimal aspect ratios are typically in the range $0.5 \le \Lambda_0 \le 1$ in order to minimize the effects of either an initial ‘reverse squeeze flow’ when the plates are first separated (at low aspect ratios $\Lambda(t) << 1$) or sagging and bulging of the cylindrical sample (at high aspect ratios). The final aspect ratio $\Lambda_f = h_f/2R_0$ attained when the plates are separated controls the total Hencky strain that is applied and is discussed further below.

The Capillary Length: $l_{cap} = \sqrt{(\sigma/\rho g)}$
Surface tension is employed in order to hold the initial fluid sample between the two endplates.

It is thus essential that the initial plate separation h_O is small enough to support a static liquid bridge. Although the classical Plateau-Rayleigh stability criterion $h_O \leq 2\pi R_O$ is well-known [34, 35], this result only applies in the absence of buoyancy forces. For the case of axial gravity, the situation is more complex and the maximum stable sample size depends on both the fluid volume and the Bond number $Bo = \rho g R_O^2/\sigma$ [36]. In order to keep the initial configuration close to cylindrical (with little axial 'sagging') capillary breakup tests typically employ axial separations $h_O \leq l_{cap}$ or equivalently $h_O/R_O \leq 1/\sqrt{Bo}$. For water (ρ = 1000 kg/m^3; σ = 0.072 N/m), the capillary length is l_{cap} = 2.7mm.

The Viscous Break-up Timescale: t_V

For a viscous Newtonian fluid undergoing capillary thinning, a simple force balance shows that the break-up process proceeds linearly with time [37]; and close to break-up the filament profile is found to be self-similar [38 - 40]. These observations can be combined to provide a means of extracting quantitative values for the capillary velocity $v_{cap} = \sigma/\mu$, or correspondingly the fluid viscosity (if the surface tension is determined independently). Provided gravitational effects are not important (so that $R_{mid} << l_{cap}$), the evolution in the midpoint radius is given by McKinley and Tripathi [5]:

$$R_{mid}(t) = R_o - \frac{\sigma}{14.1\mu}t \tag{4}$$

The characteristic viscous time scale for the break-up process is thus $t_V = 14.1\,\mu R_O/\sigma$.

The Rayleigh Time Scale: t_R

For a "low viscosity fluid" (to be defined more precisely below), the linear stability analysis of Lord Rayleigh [35] for break-up of an inviscid fluid jet is an appropriate starting point. Dimensional analysis shows that the characteristic time scale arising in inertio capillary processes is a time constant now defined as the Rayleigh time, $t_R = \sqrt{(\rho R_O^3/\sigma)}$. For a filament or jet of water with radius 3mm, the Rayleigh time scale is extremely short, t_R = 0.02 s (20 ms), so that necking and rupture proceeds extremely rapidly. This time scale plays a key role in controlling the operability of filament thinning devices as we show below in the Discussion section.

The question that naturally arises in a capillary-thinning test is what constitutes a "low viscosity" or, conversely, a "high viscosity" fluid? This can be answered by considering the similarity solutions obtained in the past decade for the nonlinear evolution and rupture of viscous and inviscid liquid threads. Specifically we wish to compare the time scale for viscocapillary breakup, t_V, to the critical time for necking and breakup of an inviscid fluid thread which we shall denote t_i. The similarity solution for inertiocapillary pinching of a liquid thread is nonlinear in time, and of the form [40, 41]:

$$R_{mid}(t) = 0.64(\sigma/\rho)^{1/3}(t_i - t)^{2/3} \tag{5}$$

This expression is in good agreement with experimental measurements of drop pinchoff [27, 40]. The critical time to breakup is found by setting the radius $R_{mid}(t = 0) = R_O$ to give

$$t_i = \left(0.64^{-3/2}\right)\left(\frac{\rho R_o^3}{\sigma}\right)^{1/2} = 1.95 t_R \tag{6}$$

The resulting ratio of time to breakup for the visco-capillary and inertio-capillary processes is related to a dimensionless number known as the *Ohnesorge number:*

$$\frac{\textit{Viscous Time Scale}}{\textit{Inertial Time Scale}} = \frac{t_v}{t_i} = \frac{14.1\mu R_o/\sigma}{1.95\left(\rho R_o^3/\sigma\right)^{1/2}} = 7.23\,Oh \tag{7}$$

Note that here we have retained the numerical factors obtained from the similarity solutions for visco-capillary and inertio-capillary breakup in the definition. Neglecting these factors leads to quantitative errors in the viscosity obtained from observations of filament thinning [7, 42] and an inaccurate estimate for the relative balances of terms controlling capillary break-up processes. A "low-viscosity fluid" in terms of capillary breakup elongational rheometry thus implies $t_V < t_i$ (i.e. $Oh < (7.23)^{-1}$); for aqueous solutions (with $\sigma \approx 0.07$

N/m; $R_O \approx 3$ mm) this corresponds to $\mu < 0.063$ Pa s.

The Opening Time δt_O and the Imposed Axial Strain ϵ_f

In a torsional step strain experiment, the shear strain is considered theoretically to be applied instantaneously. In reality, the step response of a conventional torsional rheometer is on the order of 25 - 50 ms and the torsional displacement is approximately linear with time. By analogy, the axial step strain imposed during a capillary break-up test is typically considered in a theoretical analysis to be imposed instantaneously. In experiments, however, the plate separation occurs in a finite time, denoted δt_O. If a servo-system is used to stretch the liquid filament, then this time can be varied and the displacement profile may be linearly or exponentially increasing with time. However, as a result of inertia in the plate & drive subsystem it typically is constrained to be $\delta t_O \geq 0.050$ s. Because the filament must not break during the opening process we must require $t_v \geq \delta t_O$. This criterion sets a stringent lower bound on the Newtonian viscosity that can be tested in a CABER device as we show below.

The initial rapid separation of the endplates also results in the imposition of an initial Hencky strain (a 'pre-strain') of magnitude $\epsilon_f = ln(h_f/h_O) = ln(\Lambda_f/\Lambda_O)$. As a consequence of the no-slip boundary conditions, the deformation of the fluid column is not homogeneous (i.e. the sample does not remain cylindrical); this axial measure of the strain is thus not an accurate measure of the actual Hencky strain experienced by fluid elements near the midplane of the sample. If the initial radius of the sample at time t_O is R_O and the midpoint radius of the filament at time $t_1 = t_O + \delta t_O$ is denoted R_1, then the true Hencky prestrain imposed during the stretching process is $\epsilon_1 = 2ln(R_O/R_1)$. It is not possible to predict this final radius R_1 without choosing a constitutive model for the fluid; however, for many test samples (with $t_v >> \delta t_O$), the midpoint radius of the sample at the cessation of the stretching is given by the lubrication solution for a viscous Newtonian fluid [43]:

$$R_1 \approx R_o \left(L_f / L_o\right)^{-3/4} \tag{8}$$

The Polymer Relaxation Time: λ

If the test fluid in a capillary thinning test is a polymer solution, then non-Newtonian elastic stresses grow during the transient elongational stretching process. Ultimately these extensional stresses grow large enough to overwhelm the viscous stress in the neck. An elastocapillary force balance on a uniform cylindrical thread of radius R_1 then predicts that the filament radius decays exponentially in time:

$$\frac{R_{mid}(t)}{R_1} = \left(\frac{GR_1}{2\sigma}\right)^{1/3} \exp\left[-t/3\lambda\right] \tag{9}$$

The additional factor of $2^{-1/3}$ in the prefactor of Eq. 9 is missing in the original theory [37] due to a simplifying approximation made in deriving the governing equation [26]. This simplification however does not change the exponential factor that is used to measure the characteristic time constant of the polymeric liquid. This exponential relationship between the neck radius and time has been utilized to determine the relaxation time for many different polymeric solutions over a range of concentrations and molecular weights [3, 4, 6, 7, 42]

Note that although this time constant is referred to as a 'relaxation time' – because it is the same time constant that is associated with stress relaxation following cessation of steady shear – in a capillary-thinning experiment, the stress is not relaxing *per se*. In fact the tensile stress diverges as the radius decays to zero. The time constant obtained from a CABER test is thus more correctly referred to as the 'characteristic time scale for viscoelastic stress growth in a uniaxial elongational flow'. This is, of course, precisely the time constant of interest in commercial operations concerned with drop break-up, spraying, mold-filling, etc.

For low viscosity systems, however, this exponential decay becomes increasingly difficult to observe due to the formation of the well-known beads-on-a-string morphology [23, 24]. The elastic stresses in the necking filament grow on the characteristic scale λ and must grow sufficiently large to resist the growth of free-surface perturbations, which evolve on the Rayleigh time scale, t_R. In the same manner that comparison of the viscous and Rayleigh time scales resulted in a dimensionless group (the Ohnesorge number) so too does comparison of the polymer time scale and the Rayleigh time scale. This dimensionless ratio may truly be thought of as a Deborah number [44] because it compares the magnitude of the polymeric time scale with the flow time scale for the necking process in a low viscosity fluid:

$$De \equiv \frac{\lambda}{t_R} = \frac{\lambda}{\sqrt{\rho R_o^3/\sigma}} \tag{10}$$

Note however that because the necking filament is not forced by an external deformation, it selfselects the characteristic time scale for the necking process. This Deborah number is thus an 'intrinsic quantity' that cannot be affected by the rheologist; except in so far as changes in the concentration and molecular weight of the test fluid change the characteristic time constant of the fluid.

This is not the only possible dimensionless measure of viscoelastic effects. The deformation rate in an exponentially-necking thread is given (using Eq. 9) by $\dot{\epsilon} \equiv -(2/R_{mid})dR_{mid}/dt = 2/(3\lambda)$. The product of the relaxation time and the deformation rate is thus a constant that may be defined as a Weissenberg number, $Wi \equiv \lambda\dot{\epsilon} = 2/3$. As noted by Entov and Hinch [37], this value exceeds the critical value $Wi = 1/2$ for the coil stretch transition in uniaxial flow in order to maintain the squeezing flow and ensure the elastic stress balances the ever-growing capillary pressure. However, once again this value can not be externally varied and is determined by the polymer relaxation time and the fluid surface tension.

As we have shown above the Rayleigh timescale is very small for aqueous polymer solutions. Inertio-capillary thinning thus results in rapid stretching in the fluid filament with local strain rates on the order of $\dot{\epsilon} \sim t_R^{-1} \geq 50 s^{-1}$. It should thus be possible to test low viscosity fluids with small relaxation time constants. The question is how small? In the experiments described below, we seek to determine for what range of Deborah numbers it is possible to use capillary breakup extensional rheometry to determine the relaxation time of low viscosity fluids.

3 RESULTS

3.1 BEADS ON A STRING AND INERTIO-CAPILLARY OSCILLATIONS

In Fig. 2 we present a sequence of digital video images that demonstrate the time evolution in the filament profile for the 0.10 wt% PEO solution; corresponding to a very low Deborah number, $De = 0.072$. In all of the experiments presented in this paper we define the time origin to be the instant at which axial stretching ceases, so that $t = t_{lab} - \delta t_0$. The first image at time $t = -0.05$ s thus corresponds to the initial configuration, of the liquid bridge with $\Lambda_0 = 3$ mm/6 mm = 0.5. We also report the total time for the break-up event to occur as determined from analysis of the digital video sequence; with the present optical and lighting configuration the uncertainty in determining the break-up time is approximately ± 0.005 s. For consistency we then show a sequence of five images that are evenly spaced throughout the break-up process. The horizontal shaded region indicate the approximate width of the laser light sheet that is projected by the laser micrometer.

From Fig. 2, it is clear that initially, during the first 25 ms of the axial stretching phase, the filament profile remains almost axially-symmetric about the midplane and a neck starts to form near the middle of the fluid thread as expected. However, this axial symmetry is not maintained at the end of the stretching sequence and a local defect or 'ligament' forms near the lower plate. Following the cessation of stretching, the filament rapidly evolves into a characteristic beads-on-a-string structure with a primary droplet and several smaller 'satellite droplets'. The hemispherical blobs attached to each end plate oscillate with a characteristic time

Figure 2: Formation of a beads-on-string and droplet in the 0.1% PEO fluid filament for $\Lambda = 2.0$ and $h_o = 3$ mm, in which $t_{event} = 50$ ms.

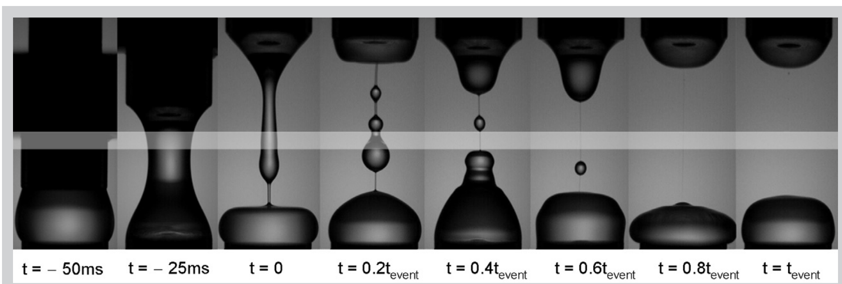

scale that is proportional to the Rayleigh time constant, t_R = 22 ms.

The strong top-bottom asymmetry in the axial curvature that can be observed in the thin ligament which develops at t = 0 is a hallmark of an inertially-dominated break-up process [39, 45]; the viscous time-scale is only t_v = 1.6 ms for this low viscosity fluid, hence we find $Oh \ll 1$ and the absence of an axially-uniform filament near the midplane suggests additionally that elastic effects are weak and $De \ll 1$. It is thus not easy to use such experiments to extract the viscoelastic time constant of the fluid. Elastic stresses only become important on very small length scales and very short time scales when the stretching rate associated with Rayleigh break-up becomes sufficiently large. From Eq. 10 we may estimate this length scale by equating the polymeric and inertial (Rayleigh) time scales (i.e. by setting $De \approx 1$) to find $R_{ligament} \sim (\lambda^2\sigma/\rho)^{1/3}$. Conversely, the effective relaxation time may be estimated from observing the size of the viscoelastic ligament that initially forms when elastic effects first become important. From Fig. 2c we estimate $R_{ligament} \approx$ 0.3mm, thus indicating that $\lambda = (\sigma R_{ligament}{}^3/\rho)^{1/2} \approx$ 1 ms. Such a measurement is clearly imprecise; but serves to provide an *a priori* estimate that can be used to compare with better measurements we make below.

A second example of difficulties that can be encountered with CABER measurements is shown in Fig. 3 for the 0.1 wt% PEO solution in water/glycerol. The increased viscosity of the fluid delays the break-up event substantially and the increased relaxation time of the polymer leads to the formation of an axially uniform fluid ligament as desired. However, inertial oscillations of the hemispherical droplets attached to each endplate still occur. The low aspect ratio of the selected test configuration (h_f = 8.46 mm; Λ_f = 1.41) results in these oscillations intruding into the observation plane of the laser micrometer. The period of these fluctuations may be estimated from the Rayleigh theory for oscillations of an inviscid liquid drop (see Chandrasekhar, 1962 for additional details). The fundamental mode has a period $t_{osc} \equiv 2\pi/\omega_{osc} = (\pi/\sqrt{2})t_R$. For the 0.1 wt% PEO solution this gives $t_{osc} \approx$ 46 ms in good agreement with the experimental observations.

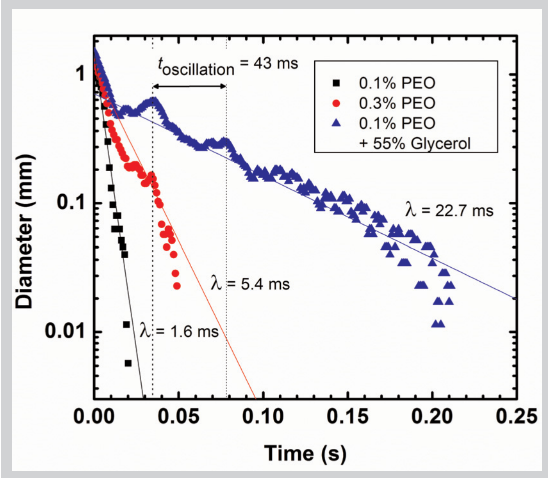

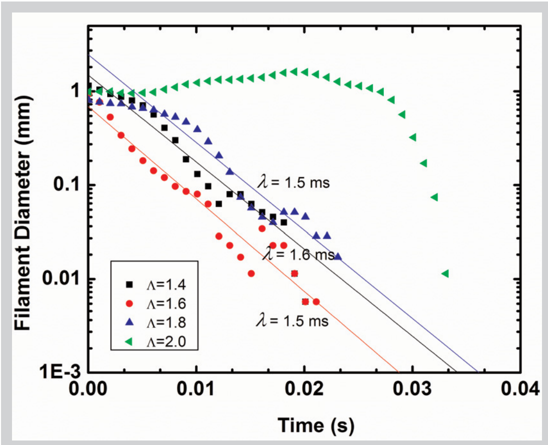

Figure 4: Exponential decay of the fluid filament diameter for a (right above) 0.1% PEO, 0.3% PEO and 0.1% PEO/glycerol solutions at an aspect ratio of 1.41, and b (right middle) 0.1% PEO solution for h_o = 3mm and Λ = 1.41, 1.61, 1.79 and 2.

The consequences can be seen in Fig. 4a which shows the evolution in the midpoint diameter $D_{mid}(t) = 2R_{mid}(t)$. The oscillations can be clearly seen in the data for the 0.1 wt% glycerol/water solution; however the exponential decay in the radius at long times can still be clearly discerned; and the data can be fitted to a decaying exponential of the form given by Eq. 9. The value of the characteristic time constant for each measurement is shown on the figure. The lower viscosity 0.1 wt% and 0.3 wt% solutions break very rapidly; typically within the period of a single oscillation.

The effects of varying the imposed stretch, i.e. varying the final aspect ratio $\Lambda_f = h_f/2R_o$, on the evolution of the midplane diameter is shown in Fig. 4b. At the highest aspect ratio (Λ_f = 2), corresponding to the high-speed digital images shown in Fig. 2, the measurements do not show

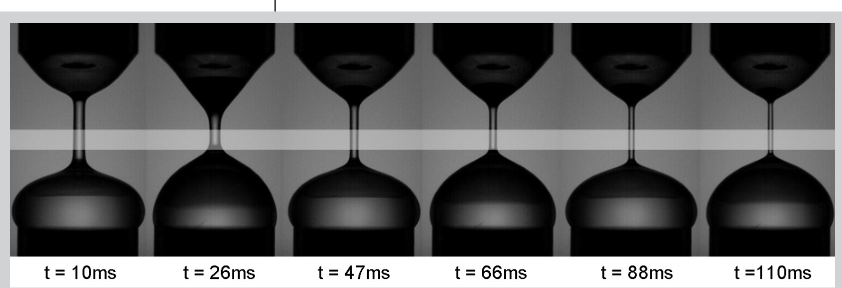

Figure 3 (left below): Periodic growth and thinning of the filament diameter due to the inertial oscillation of the fluid end-drops seen in the 0.1% PEO/glycerol solution at early times, for Λ = 1.41 and h_o = 3 mm.

exponential thinning behavior as a consequence of the large liquid droplet passing through the measuring plane. As the aspect ratio is decreased, the data begins to approximate exponential behavior and regression of Eq. 9 to the data results in reasonable estimates of the relaxation time.

3.2 SAMPLE SIZE AND VOLUME

As we noted above in Section 2, the initial sample configuration can play an important role in ensuring that capillary break-up rheometry yields reliable and successful results. By analogy, in conventional torsional rheometry it is key to ensure that the cone angle of the fixture is sufficiently small or that the gap separation for a parallel plate fixture is in a specified range. In Figs. 5 - 7 we show the consequences of varying the initial sample gap height, as compared to the capillary length $l_{cap} = \sqrt{(\sigma/\rho g)}$. In each test we use the 0.30 wt% PEO solution and a fixed final aspect ratio of Λ=1.61; corresponding to a final stretching length h_f = 1.61(2R_O) = 9.7 mm.

If h_O/l_{cap} < 1 then the interfacial force arising from surface tension is capable of supporting the liquid bridge against the sagging induced by the gravitational body force. Consequently the initial sample is approximately cylindrical and the initial deformation results in a top-bottom symmetric deformation and the formation of an axially-uniform ligament at t = 0 when deformation ceases, as shown in Fig. 5. However, if the initial gap is larger, as shown in Fig. 6 (corresponding here to h_O = 3mm) and exceeds the capillary length scale (h_O/l_{cap} = 1.19), then asymmetric effects arising from gravitational drainage become increasingly important. Even under rest conditions (as shown by the first image in Fig. 6), gravitational effects result in a detectable bulging in the lower half of the liquid bridge; as predicted numerically [36]. This asymmetry is amplified during the 'strike' or gap-opening process as indicated in the 2nd and 3rd frames. However as viscoelastic stresses in the neck region grow and a thin elastic thread develops, the process stabilizes and exponential filament thinning occurs once again. In Figure 7 we show an even more pronounced effect when the initial gap is 4 mm (corresponding to h_O/l_{cap} = 1.58). The asymmetry of the initial condition and the extra fluid volume (corresponding to a volume of $V \approx \pi R_O{}^2 h_O$ = 113 μl; i.e. twice the fluid volume in Fig. 5) is sufficient to initialize the formation of a 'bead' or droplet near the middle of the filament at t = 25 ms (0.2t_{event}), which subsequently drains into the lower reservoir. A distinct uniform axial thread only develops for times greater than $t \geq 0.3t_{event} \approx$ 0.04 s. This severely limits the useful range of measurements.

The measured midpoint diameters for the conditions in Figs. 5 - 7 are shown in Fig. 8. The progressive drainage of the primary droplet through the measuring plane of the laser

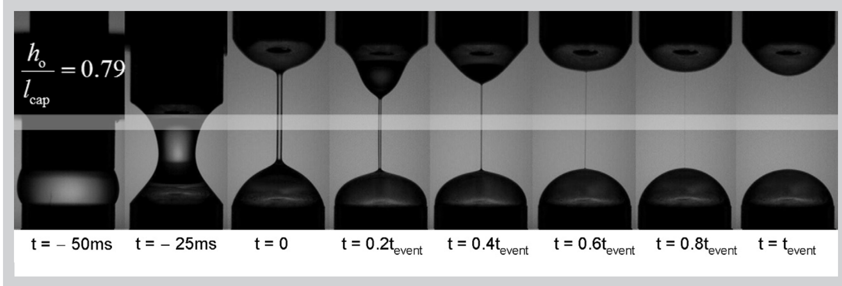

Figure 5 (above): Filament thinning of the 0.3% PEO solution for an initial gap height of h_o = 2 mm and Λ = 1.61, in which the total time of the event, t_{event} = 100 ms.

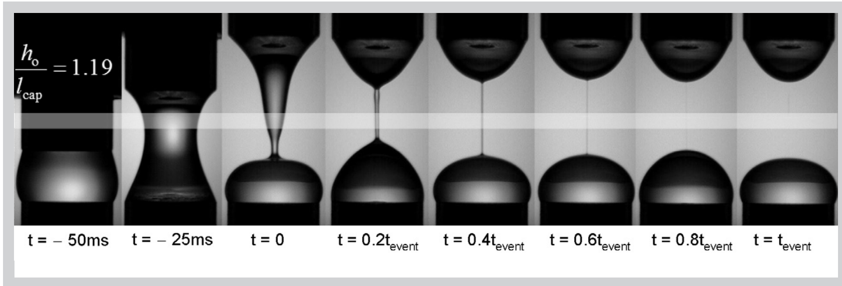

Figure 6 (middle): Filament thinning of the 0.3% PEO solution for an initial gap height of h_o = 3 mm and Λ = 1.61, in which the total time of the event, t_{event} = 110 ms.

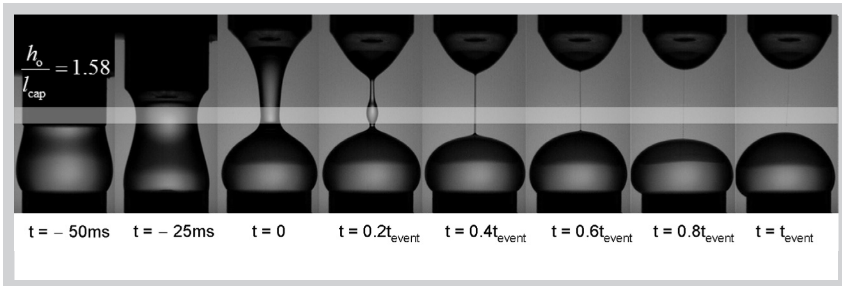

Figure 7 (below): Filament thinning of the 0.3% PEO solution for an initial gap height of h_o = 4 mm and Λ = 1.61, in which the total time of the event, t_{event} = 125 ms.

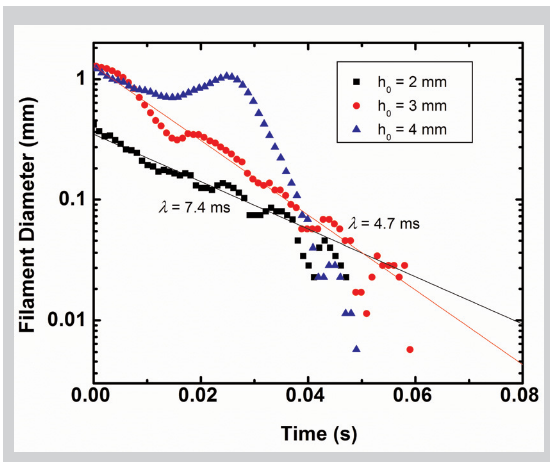

Figure 8: Exponential decay of the fluid filament diameter for the 0.3% PEO solution for Λ = 1.6 and initial sample heights of h_o = 2, 3 and 4 mm.

micrometer can be clearly seen in the data for h_o = 4 mm. Although an exponential regime (corresponding to elasto-capillary thinning with approximately constant slope of the form given by Eq. 9) can be seen for the intermediate separation (h_o = 3 mm), the effects of the initial asymmetry in the sample – coupled with the perturbing effects of axial drainage during the plate separation – result in fluctuations in the diameter profile and an under-prediction in the longest relaxation time. The smallest initial gap setting (h_o = 2 mm), however, results in steady exponential decay over a time period of approximately Δt = 40 ms; corresponding to $\Delta t/3\lambda \approx 1.8$ and, consequently from Eq. 9 a diameter decrease of more than a factor of 6. This is of a sufficiently wide range to satisfactorily regress to the equation.

One important feature to note from a careful comparison of Figs. 7 and 8 is the difference in spatial resolution offered by the digital imaging system; the laser micrometer has a calibrated spatial resolution of ca. 20 μm [6] which is reached after a time interval of approximately $\Delta t \approx 50$ ms; hence $\Delta t/t_{event} \approx 50/125 = 0.4$. By contrast, a thin elastic ligament can still be visually discerned for another 50 ms. The performance of future Capillary Break-up Extensional Rheometers may thus be enhanced by employing laser micrometers with higher spatial resolution or using analog/digital converters with 16 bit or 20 bit resolution. Such devices however typically become increasingly bulky and expensive.

3.3 THE ROLE OF FLUID VISCOSITY AND ASPECT RATIO

As we noted in Section 2.1, the longest relaxation time and also the zero-shear rate viscosity of a dilute polymer solution both vary with the viscosity of the background Newtonian solvent and also with the concentration of the polymer in solution. The characteristic viscous and elastic time scales associated with the break-up process also increase and so do the dimensionless parameters *Oh* and *De*. Inertial effects thus become progressively less important and capillary break-up experiments become concomitantly easier. An example is shown in Fig. 9 for the 0.1 wt% PEO solution in glycerol/water at a high aspect ratio (Λ_f = 2.0). The equivalent process in a purely aqueous solvent has already been shown in Fig. 2 and resulted in a beads-on-string structure that corrupted CABER experiments. However, by increasing the background solvent viscosity this break-up process is substantially retarded (the total time for break-up increases from 50 ms to over 400 ms) and a uniform fluid filament is formed between the upper and lower plates. The corresponding midpoint diameter measurements for each of the test fluids (in this case with a reduced aspect ratio of Λ_f = 1.6 and an initial gap of h_o = 3mm) are shown in Fig. 10a. For the 0.1 wt% PEO solution in glycerol/water a statistically significant deviation from a pure exponential decay can be observed for $t \geq 0.18$s. Theoretical considerations show that this deviation should correspond to the onset of finite extensibility effects associated with the PEO molecules in the stretched elastic ligament attaining full

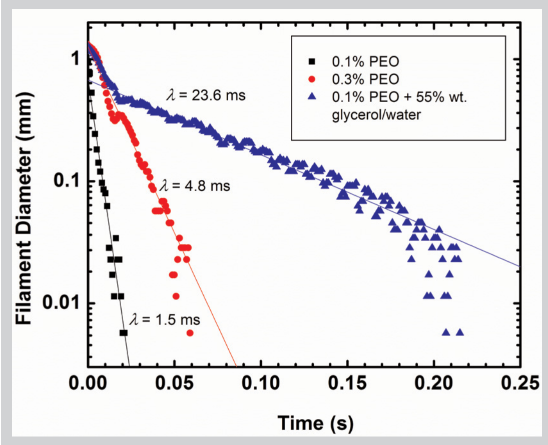

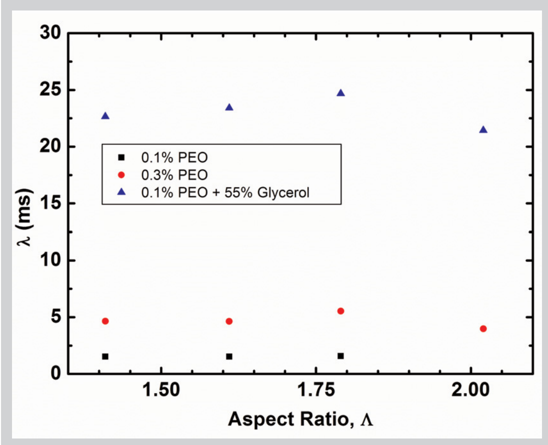

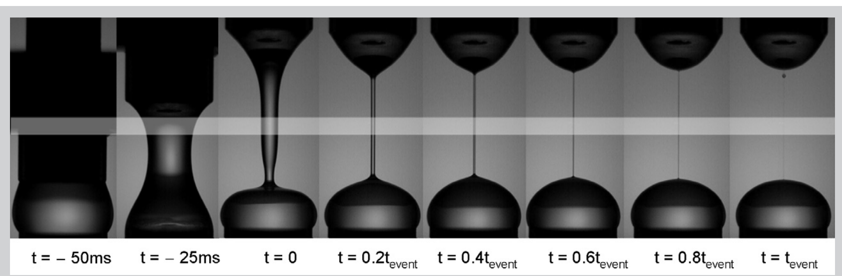

Figure 9 (left below): Thinning of fluid filament for the 0.1% PEO/glycerol solution for Λ = 2 and h_o = 3 mm, in which the total event time, t_{event} = 420 ms.

Figure 10: a (right above): Exponential decay of the fluid filament diameter for Λ=1.61 and h_o = 3mm and b (right middle): relaxation time as a function of aspect ratio, for the 0.1% PEO, 0.3% PEO and 0.1% PEO/ glycerol solutions in which h_o = 3mm.

extension [37]. In this final stage of break-up, numerical simulations with both the FENE-P and Giesekus models show that the filament radius decreases linearly with time [46].

Finally, our results for the measured relaxation times of the three test fluids are summarized in Fig. 10b. Each point represents the average of at least three tests under the specified experimental conditions. No data could be obtained with the 0.1 wt% PEO/water solution at aspect ratios $\Lambda \geq 1.8$ due to the inertio-capillary break-up and beads-on-a-string morphology shown in Fig. 2. It can be noted that the measured relaxation times vary with aspect ratio only very weakly. This is reassuring for a rheometric device and indicates that relaxation times as small as $\lambda \approx 1$ ms can successfully be measured using capillary thinning and break-up experiments. Average values of the measured relaxation times are tabulated in the final column of Table 1.

We have also investigated the role of dynamical variations in the surface tension by repeating the experiments in the 0.1 wt% glycerol/water solution after addition of 0.4% 2-butanol. Dynamic surface tension measurements using a maximum bubble volume tensiometer show that this small molecule migrates to the interface very rapidly (in less than 1 ms) and leads to a surface tension coefficient that is constant over the time of the breakup process [27]. Capillary breakup measurements show that the relaxation time remains essentially unchanged with mean values (n = 5) of λ = 18 ± 1 ms (no butanol added) to 17 ± 1 ms (with 0.4% 2-butanol added).

4 DISCUSSION & CONCLUSION

In this paper we have performed capillary break-up extensional rheometry (CABER) experiments on a number of semi-dilute polymer solutions of varying viscosities using cylindrical samples of varying initial size and imposed stretches of different axial extent leading to various imposed axial strains. High speed digital imaging shows that changes in these parameters may change the dynamics of the filament thinning and break-up process for each fluid substantially.

By considering the natural length scales and time scales that govern these dynamics, we have been able to develop a number of dimensionless parameters that control the successful operability of such devices as extensional rheometers; the most important being the Ohnesorge number and a natural or 'intrinsic' Deborah number. In addition, decreasing the Bond number, or equivalently the dimensionless aspect ratio $h_0/R_0 \leq 1/\sqrt{Bo}$, can help extend the operating range by minimizing the effects of gravitational drainage. These constraints can perhaps be most naturally represented in the form of 'operability diagrams' such as the ones sketched in Figure 11. In Fig. 11a we select the dimensional parameters corresponding to the zero-shear-rate viscosity, η_0, of the solution and the characteristic relaxation time, λ, as the abscissa and ordinate axes respectively. A more general version of the same nomogram is shown in Fig. 11b in terms of the Ohnesorge and Deborah numbers.

For Newtonian fluids (corresponding to $\lambda = 0$) we require, at a minimum, that $t_v \geq t_i$ (or equivalently from Eq. 7 that $Oh \geq 7.23^{-1} \approx 0.14$) in order to observe the effects of fluid viscosity on the local necking and break-up. As we discussed in Section 2.3 for the present configuration this gives a lower bound on the measurable viscosity of 63 mPa s. However, the device also takes a finite time (which we denote δt_0) to impart the initial axial deformation to the sample. An additional constraint is thus $t_v \geq \delta t_0$ or

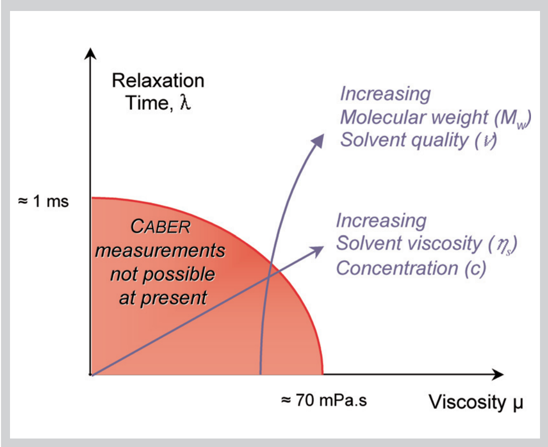

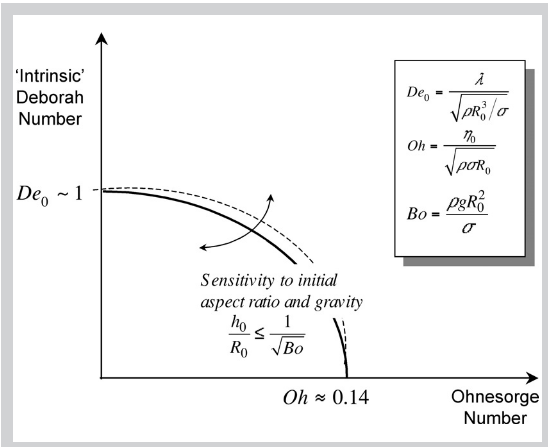

Figure 11: An 'operability diagram' for capillary break-up elongational rheometry.
a (above): dimensional form showing the minimum values of viscosity, μ, and relaxation time, λ, required for successful measurement of the capillary thinning with presently available instrumentation;
b (below): dimensionless form of the nomogram showing fundamental limitations to the operation of such devices.

$$\mu \geq \frac{\sigma}{14.1R_o}\delta t_o$$

For a prototypical Newtonian fluid with $\sigma \approx 0.060$ N/m, a plate size of $R_o = 3$mm and an opening time of $\delta t_o = 50$ms we find $\mu \geq 0.071$ Pa s. This defines the intersection of the operability boundary with the abscissa. Increasing the displacement rate of the linear motor in order to reduce the opening time would enable somewhat lower viscosity fluids to be tested; however the critical time scale t_i for inerto-capillary break-up of a Newtonian fluid thread will ultimately limit the range of viscosities that can be successfully tested.

The dilute polymer solutions tested in the present study obviously have viscosities significantly less than this value, and viscoelasticity further stabilizes the filament against breakup. The simplest estimate for the range of relaxation times that can be measured is to require that the intrinsic Deborah number is of order unity, or equivalently $\lambda \geq t_R = \sqrt{(\rho R_1^3/\sigma)} \approx 6$ ms. However this estimate is based on an elasto-capillary balance in the thread of radius R_1 that is formed at the instant that the imposed stretching ceases (see Eq. 8). In reality we are able to resolve thinning threads of substantially smaller spatial scale. Closer analysis of the digital video from which the images in Fig. 2 are taken (specifically, the frames between times $t = -25$ ms and 0 ms which are not presented here) shows that a neck first forms at $t = -5$ ms, when the thread diameter at the neck is approximately 200μm; the minimum resolvable viscoelastic relaxation time should thus be $\lambda >> \sqrt{((10^3)(2 \cdot 10^{-4})^3/(0.06))} \approx 0.4$ ms.

However, just as in the above arguments regarding the minimum measurable Newtonian viscosity, the capabilities of the instrumentation also play a role and may serve to further constrain the measurable range of material parameters. More specifically, the minimum measurable radius, the total imposed stretch and the sampling rate will all impact the extent to which a smoothly decaying exponential of the form required by Eq. 9 can be resolved. In the present experiments we have sampled the analog diameter signal from the laser micrometer at a rate of 1000 Hz ($\delta t_s = 0.001$s), and the minimum radius that can be reliably detected by the laser micrometer is $R_{min} \approx 20$ μm. If we require that, as an absolute minimum, we monitor the elastocapillary thinning process long enough to obtain 5 points that can be fitted to an exponential curve, then the measured radius data must span the range $R_{min} \leq R_{mid}(t) \leq R_{min}e^{+5\delta t_s/3\lambda}$. However the radius of the neck at the cessation of the imposed stretching ($t = 0$) is given (at least approximately) by Eq. 8. Combining these expressions we thus require that

$$R_{\min}e^{5\delta t_s/3\lambda} \leq R_1 = R_o\left(\Lambda_f\right)^{-3/4}$$

Rearranging this expression gives:

$$\lambda \geq \frac{5\delta t_s/3}{\ln\left[R_o\Lambda_f^{-3/4}/R_{\min}\right]} \tag{11}$$

For an axial stretch of $\Lambda_f = 1.6$, a sampling time of 1 ms, and a minimum detectable radius of 20 μm we obtain a revised estimate of the minimum measurable relaxation time $\lambda \geq 0.36$ ms, which is in agreement with our present observations. In reality, Eq. 8 is an overestimate of the neck radius, R_1, at the cessation of the stretching phase, since the lubrication theory from which it is derived implicitly assumes viscous effects are fully developed throughout the axial stretching process. The data in Fig. 4 show that, in general, for low viscosity fluids the exponential necking phase starts at a somewhat lower value of the measured radius. This will increase the lower bound given by Eq. 11; however the weak logarithmic dependence of this expression on the precise value of the radius makes such corrections small.

This estimate of the minimum viscoelastic time scale denotes the limiting bound of successful operation for a very low viscosity (i.e. an almost inviscid) elastic fluid; corresponding to the ordinate axis ($Oh \longrightarrow 0$) of Fig.11. The shape and precise locus of the operability boundary within the two-dimensional interior of this parameter space will depend on all three time scales (viscous, elastic and inertial) and also on the initial sample size (h_o/l_{cap}) and the total axial stretch, Λ_f, imposed. It thus needs to be studied in detail through numerical simulations. However, our experiments indicate that it is possible, through careful selection of both the initial gap, h_0, and the final strike distance, h_f, to successfully measure relaxation times as small as 1 ms for low viscosity elastic fluids with zero-shear-rate viscosities as small as 3 mPa s. Near the boundary of the operating space it is important to perform multiple experiments in order to obtain reliable measures of the mean value and standard deviations of the measured relaxation times. By analogy, in shear rheometry of low viscosity fluids it is essential to perform multiple experiments and average the measured stress signal in order to obtain reliable values of the viscometric properties.

A final practical use of an 'operability diagram' such as the one sketched in Fig. 11 is that it enables the formulation chemist and rheologist to understand the consequences of changes in the formulation of a given polymeric fluid. The changes in the zero-shear-rate viscosity and longest relaxation time that are expected from dilute solution theory and formulae such as Eq. 3 are indicated by the arrows. Increases in the solvent quality and molecular weight of the solute lead to large changes in the relaxation time, but small changes in the overall solution viscosity (at least under dilute solution conditions). By contrast, increasing the concentration of dissolved polymer into the semi-dilute and concentrated regimes leads to large increases in both the zero-shear-rate viscosity and the longest relaxation time. It should be noted that the dynamics of the break-up process can change again at very high concentrations or very high molecular weights when the solutions enter the entangled regime (corresponding to $cM_w \geq \rho M_e$, where M_e is the entanglement molecular weight of the melt). Although capillary thinning and break-up experiments can still be successfully performed, the dimensionless filament lifetime t_{event}/λ (as expressed in multiples of the characteristic relaxation time) may actually decrease from the values observed in the present experiments due to chain disentanglement effects [47]; i.e. a concentrated polymer solution may actually be less extensible than the corresponding dilute solution. Capillary thinning and break-up experiments of the type described in this article enable such effects to be systematically probed.

REFERENCES

[1] Dontula P, Pasquali M, Scriven LE, Macosko CW: Model Elastic Liquids with Water-Soluble Polymers, AIChE J. 44 (1998) 1247-1256.

[2] Harrison GM, Boger DV: Well-Characterized Low Viscosity Elastic Liquids, Appl. Rheol. 10 (2000) 166-177.

[3] Bazilevsky AV, Entov VM, Rozhkov AN: Liquid Filament Microrheometer and Some of its Applications, Third European Rheology Conference, Oliver DR (ed.), Elsevier Applied Science (1990).

[4] Bazilevskii AV, Entov VM, Lerner MM, Rozhkov AN: Failure of Polymer Solution Filaments, Polymer Science Ser. A 39 (1997) 316-324 (translated from Vysokomolekulyarnye Soedineniya Ser. A).

[5] McKinley GH, Tripathi A: How to Extract the Newtonian Viscosity from Capillary Breakup Measurements in a Filament Rheometer, J. Rheol. 44 (2000) 653-671.

[6] Anna SL, McKinley GH: Elasto-capillary Thinning and Breakup of Model Elastic Liquids, J. Rheol. 45 (2001) 115-138.

[7] Stelter M, Brenn G, Yarin AL, Singh RP, Durst F: Validation and Application of a Novel Elongational Device for Polymer Solutions, J. Rheol. 44 (2000) 595-616.

[8] Stelter M, Brenn G, Yarin AL, Singh RP, Durst F: Investigation of the Elongational Behavior of Polymer Solutions by Means of an Elongational Rheometer, J. Rheol. 46 (2002) 507-527.

[9] Bazilevskii AV, Entov VM, Rozhkov AN: Failure of an Oldroyd Liquid Bridge as a Method for Testing the Rheological Properties of Polymer Solutions, Polymer Science Ser. A 43 (2001) 1161- 1172 (translated from Vysokomolekulyarnye Soedineniya Ser. A.).

[10] Tripathi A, Whittingstall P, McKinley GH: Using Filament Stretching Rheometry to Predict Strand Formation and "Processability" in Adhesives and Other Non-Newtonian Fluids, Rheol. Acta 39 (2000) 321-337.

[11] Willenbacher N: Elongational Viscosity of Aqueous Thickener Solutions from Capillary Breakup Elongational Rheometry (CaBER), Proceeding of the XIVth International Congress on Rheology, Seoul (2004).

[12] McKinley GH: A Decade of Filament Stretching Rheometry, Proceeding of the XIIIth International Congress on Rheology, DM Binding et al. (Eds.), Cambridge (2000) 15-22.

[13] McKinley GH: Visco-Elasto-Capillary Thinning and Breakup of Complex Fluids, Rheology Reviews 3 (2005) to appear.

[14] Fuller GG, Cathey CA, Hubbard B, Zebrowski BE: Extensional Viscosity Measurements for Low Viscosity Fluids, J. Rheol. 31 (1987) 235-249.

[15] Hermansky CG, Boger DV: Opposing-Jet Viscometry of Fluids with Viscosity Approaching That of Water, J. Non-Newtonian Fluid Mech. 56 (1995) 1-14.

[16] Ng SL, Mun RP, Boger DV, James DF: Extensional Viscosity Measurements of Dilute Polymer Solutions of Various Polymers, J. Non-Newtonian Fluid Mech. 65 (1996) 291-298.

[17] Dontula P, Pasquali M, Scriven LE, Macosko CW: Can Extensional Viscosity be Measured with Opposed-Nozzle Devices, Rheol. Acta 36 (1997) 429-448.

[18] Schümmer P, Tebel KH: A New Elongational Rheometer for Polymer Solutions, J. Non-Newtonian Fluid Mech. 12 (1983) 331-347.

[19] Christanti YM, Walker L: Surface tension driven jet break up of strain-hardening polymer solutions, J. Non-Newtonian Fluid Mech. 100 (2001) 9-26.

[20] Amarouchene Y, Bonn D, Meunier J, Kellay H: Inhibition of the Finite Time Singularity during Droplet Fission of a Polymeric Fluid, Phys. Rev. Lett. 86 (2001) 3558-2562.

[21] Cooper-White JJ, Fagan JE, Tirtaatmadja V, Lester DR, Boger DV: Drop Formation Dynamics of Constant Low Viscosity Elastic Fluids, J. Non-Newtonian Fluid Mech. 106 (2002) 29- 59.

[22] Kolte MI, Szabo P: Capillary Thinning of Polymeric Filaments, J. Rheol. 43 (1999) 609-626.

[23] Goldin M, Yerushalmi H, Pfeffer R, Shinnar R: Breakup of a Laminar Capillary Jet of a Viscoelastic Fluid, J. Fluid Mech. 38 (1969) 689-711.

[24] Li J, Fontelos MA: Drop Dynamics on the Beads-on-String Structure for Viscoelastic Jets: A Numerical Study, Phys. Fluids 15 (2003) 922-937.

[25] Neal G, Braithwaite GJC: The Use of Capillary Breakup Rheometry to Determine the Concentration Dependence of Relaxation Time, 75th Annual Meeting of the Society of Rheology, Pittsburgh (2003).

[26] Clasen C, Verani M, Plog JP, McKinley GH, Kulicke WM: Effects of Polymer Concentration and Molecular Weight on the Dynamics of Visco-Elasto-Capillary Breakup, Proceeding of the XIVth International Congress on Rheology, Seoul (2004).

[27] Tirtaatmadja V, McKinley GH, Boger DV, Cooper-White JJ: Drop Formation and Breakup of Low Viscosity Elastic Fluids: Effects of Concentration and Molecular Weight, Phys. Fluids (2004) submitted in revised form.

[28] Brandrup H, Immergut E.H: Polymer Handbook, Wiley (1997) New York.

[29] Graessley WW: Polymer Chain Dimensions and the Dependence of Viscoelastic Properties on Concentration, Molecular Weight and Solvent Power, Polymer 21 (1980) 258-262.

[30] Doi M, Edwards SF: The Theory of Polymer Dynamics, Oxford university Press (1986) Oxford.

[31] Christanti YM, Walker L: Effect of Fluid Relaxation Time on Jet Breakup due to a Forced Disturbance of Polymer Solutions, J. Rheol. 46 (2002) 733-739.

[32] Harlen OG: Simulation of the Filament Stretching Rheometer, presentation at the Isaac Newton Institute during Dynamics of Complex Fluids program (1996).

[33] Yao M: McKinley GH: Numerical Simulation of Extensional Deformations of Viscoelastic Liquid Bridges in Filament Stretching Devices, J. Non-Newtonian Fluid Mech. 74 (1998) 47-88.

[34] Plateau JAF: Experimental and Theoretical Researches on the Figures of Equilibrium of a Liquid Mass Withdrawn from the Action of Gravity, Ann. Rep. Smithsonian Institution (1863) 207-285.

[35] Rayleigh L: On the Instability of Jets, Proc. Lond. Math. Soc. 10 (1879) 4-13.

[36] Slobozhanin LA, Perales JM: Stability of Liquid Bridges between Equal Disks in an Axial Gravity Field, Phys. Fluids A 5 (1993) 1305-1314.

[37] Entov VM, Hinch EJ: Effect of a Spectrum of Relaxation Times on the Capillary Thinning of a Filament of Elastic Liquid, J. Non-Newtonian Fluid Mech. 72 (1997) 31-54.

[38] Papageorgiou DT: On the Breakup of Viscous Liquid Threads, Phys. Fluids 7 (1995) 1529-1544.

[39] Eggers J: Nonlinear Dynamics and Breakup of Free-Surface Flows, Rev. Mod. Phys. 69 (1997) 865-929.

[40] Chen AU, Notz PK, Basaran OA: Computational and Experimental Analysis of Pinch-Off and Scaling, Phys. Rev. Lett. 88 (2002) 174501-4.

[41] Day RF, Hinch EJ: Self-Similar Capillary Pinchoff of an Inviscid Fluid, Phys. Rev. Lett. 80 (1998) 704-712.

[42] Liang RF, Mackley MR: Rheological Characterization of the Time and Strain Dependence for Polyisobutylene Solutions, J. Non-Newtonian Fluid Mech. 52 (1994) 387-405.
[43] Spiegelberg SH, Ables DC, McKinley GH: The Role of End-Effects on Measurements of Extensional Viscosity in Viscoelastic Polymer Solutions With a Filament Stretching Rheometer, J. Non-Newtonian Fluid Mech. 64 (1996) 229-267.
[44] Bird RB, Armstrong RC, Hassager O: Dynamics of Polymeric Liquids. Volume 1: Fluid Mechanics, 2nd Edition, Wiley Interscience (1987) New York.
[45] Renardy M: Self-Similar Breakup of Non-Newtonian Fluid Jets, Rheology Reviews 2 (2004) 171-196.
[46] Fontelos MA, Li J: On the Evolution and Rupture of Filaments in Giesekus and FENE models, J. Non-Newtonian Fluid Mech. 118 (2004) 1-16.
[47] Bhattacharjee PK, Nguyen DA, McKinley GH, Sridhar T: Extensional Stress Growth and Stress Relaxation in Entangled Polymer Solutions, J. Rheol. 47 (2003) 269-290.